American Mineralogist, Volume 68, pages 235–244, 1983

Laffittite, $AgHgAsS_3$: crystal structure and second occurrence from the Getchell mine, Nevada

IZUMI NAKAI[1] AND DANIEL E. APPLEMAN

Department of Mineral Sciences
Smithsonian Institution
Washington, D.C. 20560

Abstract

Laffittite was found in a museum specimen labelled getchellite, from the Getchell mine, Humboldt County, Nevada. The mineral occurs in grains about 1 mm in maximum length as dark red crystals associated with orpiment, getchellite and realgar.

Laffittite, $AgHgAsS_3$, is monoclinic, space group *Aa*, $a = 7.732(3)$, $b = 11.285(7)$, $c = 6.643(4)$Å, $\beta = 115.16(3)°$, $Z = 4$. The strongest lines in the X-ray powder pattern are 3.512(100)(200), 3.202(78)(031,$\bar{1}$31), 3.015(69)(002), 2.685(67)($\bar{2}$31), 1.898(29)($\bar{1}$33,$\bar{2}$33, 2.136(18)(231,$\bar{3}$31), 3.633(16)(111), 1.889(14)($\bar{4}$11).

Single crystals were hydrothermally synthesized at 350°C under 10,000 psi pressure for 140 hours. The starting material was a fused mixture of Ag_2S, HgS and As_2S_3 having a molar ratio of 1:2:1.

The crystal structure of laffittite is a superstructure based upon the PbS structure. Metal–sulfur bonds form a hexagonal ring of one formula unit. The hexagonal rings link to each other by sharing all edges forming a sheet parallel to (100). The sheets link up and down by Hg–S and Ag–S bonds to form a three-dimensional network. As has the usual trigonal coordination by 3S (As–S = 2.26Å, avg.). Ag has (3 + 1)S coordination: Ag–S = 2.51, 2.52, 2.60 and 2.89Å. The Hg coordination group is a distorted tetrahedron: Hg–S = 2.42, 2.51, 2.71, and 2.73Å. The structure is closely related to that of marrite, $PbAgAsS_3$.

Description and synthesis

Introduction

The rare mineral laffittite, $AgHgAsS_3$, was first described by Johan *et al.* (1974) from the Jas Roux mine, Hautes Alpes, France. As far as we know, laffittite has not been reported from any other locality, and their work is the only report which has appeared on this mineral. They reported that laffittite occurred in grains up to 0.2 mm in dolomitic rock associated with routhierite, realgar, stibnite, pierrotite, smithite, sphalerite and pyrite.

During an investigation of a museum specimen from Nevada, the authors recognized a small dark red grain among getchellite crystals, and subsequent X-ray diffraction study and chemical analysis revealed it to be laffittite. We present here some mineralogical data, a method of synthesis, and new crystal data including a complete structure analysis.

Mineralogy

Laffittite was found in a Smithsonian Museum of Natural History specimen (#134796) labelled getchellite, from the Getchell mine, Humboldt County, Nevada. The specimen, about 12 × 9 × 6 cm, is a large mass of orpiment, in which getchellite veinlets are prominent. Laffittite occurs in anhedral grains about 1 mm in maximum length. The grains are usually surrounded by getchellite and/or orpiment. Other associated minerals include realgar, stibnite which is commonly observed as inclusions in orpiment, and rarely sphalerite. The typical mineral assemblage can be seen in Figure 1.

Laffittite is dark red in color and is darker than getchellite. The mineral has adamantine luster and the streak is brownish red. In reflected light in air, laffittite is clearly bireflectant, from light bluish gray with an olive tint resembling tetrahedrite, to dark bluish gray with an olive tint. Although the mineral is strongly anisotropic, this is obscured by its strong brilliant red internal reflection. These optical properties resemble those reported for laffittite in the

---

[1] Present address: Department of Chemistry, The University of Tsukuba, Ibaraki 305, Japan.

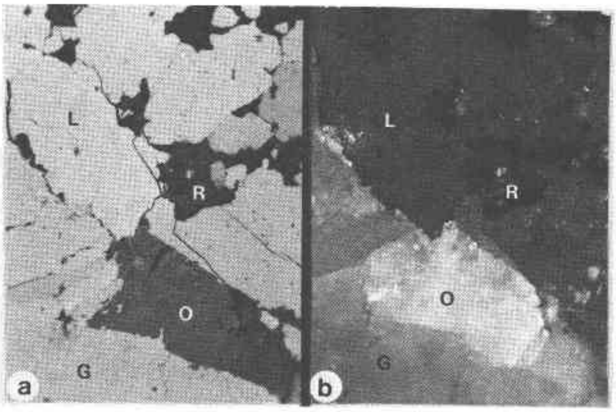

Fig. 1. Laffittite in polished section; (a) parallel polarizers, (b) crossed polarizers, L: laffittite, G: getchellite, R: realgar, O: orpiment.

original description (Johan *et al.*, 1974). Figure 1 shows a reflection microscope photograph of laffittite associated with orpiment, getchellite and realgar. Polishing hardness shows that laffittite is slightly harder than getchellite. Among the above four minerals, laffittite shows the best polishing condition, next is orpiment followed by getchellite, then realgar. The texture of this mineral assemblage does not appear to give any positive information about the formation order of these minerals. To date, no silver or mercury minerals have been found in this specimen, and the source of mercury and silver in laffittite remains in question.

Crystallography

In the original description of laffittite, Johan *et al.* (1974) reported that laffittite was monoclinic with space group $P2_1/c$; however, we have found a different symmetry. Precession photographs of laffittite crystals show monoclinic symmetry with systematic absences of $k + l = 2n + 1$ for (hkl) reflections, and $h = 2n + 1$ for $(h0l)$ reflections; thus the possible space group is $A2/a$ or Aa, and the latter is established by the crystal structure analysis.

Unit cell dimensions were first determined from precession photographs of single crystals. An attempt was made to refine these parameters by least-squares analysis of the X-ray powder data, but, as will be discussed in the section on crystal structure in this paper, the presence of a pseudocubic lattice prevented derivation of the correct cell dimensions from the powder data. The final cell parameters have been determined by single crystal measurement with the four-circle diffractometer: $a = 7.732(3)$, $b = 11.285(7)$, $c = 6.643(4)$Å, $\beta = 115.16(3)°$ (see Crystal Structure). X-ray powder diffraction data were obtained with the diffractometer method using Ni-filtered Cu$K\alpha$ radiation with a Si standard, and are given in Table 1 together with those for synthetic laffittite and those given in the original description. The indexing was accomplished with the aid of single crystal intensity data. The three X-ray powder data sets are essentially identical, although there are apparent slight differences in intensities.

Synthesis

The reagents employed were CP grade Ag_2S, HgS and As_2S_3. Starting materials for single crystal growth were synthesized by reacting a powder mixture of the above reagents having a composition ratio Ag_2S:HgS:As_2S_3 = 1:2:1 in an evacuated sealed silica tube; the mixture was held at 900°C for 12 hours and cooled slowly to 500°C and air quenched. The product is a crystalline massive material having a brownish red color. X-ray powder diffraction patterns showed that it included laffittite and cinnabar as major components and minor unidentified phases. The product was ground into fine powder in an agate motor and used as a starting material for single crystal growth.

Twenty milligrams of the starting material and 0.06 ml of either 1% Na_2S solution or 1% $Na_2B_4O_7$ solution were sealed in a gold tube (length 30 mm, inner diameter 2.7 mm). Syntheses were conducted using stellite bombs of the test tube type in the temperature range from 300°C to 400°C, 10,000 psi pressure for 140 hours.

The crystallization of laffittite was observed at any temperature between 300°C and 400°C, however syntheses at 350°C gave the best result among our experiments. Crystals synthesized are flattened hexagonal plates about 80 × 60 × 30 μm (Fig. 2). They are transparent with dark red color resembling natural laffittite. The X-ray powder diffraction patterns of the synthetic crystals agree well with that of natural laffittite; the powder data obtained by the diffractometer method are given in Table 1.

The nature of the solvent Na_2S solution or $Na_2B_4O_7$ solution, did not affect the crystallization of laffittite very much. The effect of temperature seems to be more serious: crystal growth was very slow at 300°C and only fine crystals were observed, while the crystallization of laffittite seems to be restricted above 400°C where crystallization of an

Table 1. X-ray powder diffraction data for laffittite

Laffittite from Getchell mine*				Synthetic laffittite*		Laffittite from Jas Roux mine**	
hkl	*d* calc†	*d* obs	*I/Io*	*d* obs	*I/Io*	*d* obs	*I/Io*
020	5.642	5.665	7	5.665	3		
$\bar{1}11$	5.291	5.298	13	5.298	10	5.31	50
120	4.393	4.407	13	4.407	6	4.41	30
111	3.624	3.633	16	3.633	5		
$\bar{2}11$	3.609			3.626	4	3.620	20
200	3.499	3.512	100	3.506	100	3.505	70
031	3.189	3.202	78	3.197	28	3.198	80
$\bar{1}31$	3.186						
002	3.006	3.015	69	3.011	28	3.005	80
$\bar{1}22$	2.862	2.870	7	2.867	9	2.871	10
$\bar{2}31$	2.677	2.685	67	2.683	23	2.682	100
140	2.617			2.623	2		
211	2.519					2.525	10
$\bar{3}22$	2.211	2.218	4			2.214	10
320	2.156			2.163	2		
$\bar{1}42$	2.150	2.158	7	2.154	3		
$\bar{1}13$	2.149			2.146	3		
231	2.130	2.136	18	2.135	11	2.133	60
$\bar{3}31$	2.125						
202	1.913	1.919	10	1.916	4		
$\bar{4}02$	1.905	1.911	11			1.905	50
$\bar{1}33$	1.892	1.898	29	1.892	14	1.891	50
$\bar{2}33$	1.890						
$\bar{4}11$	1.885	1.889	14	1.886	22		
160	1.816	1.823	10	1.822	5	1.822	20
033	1.769	1.774	12	1.772	5	1.771	30
$\bar{3}33$	1.764						
400	1.750	1.756	4	1.753	12		
331	1.708	1.709	10	1.708	3	1.706	40
$\bar{4}31$	1.705						
$\bar{2}04$	1.661	1.665	6	1.662	3	1.663	30
260	1.657						
$\bar{1}62$	1.637			1.640	3		
062	1.595	1.600	7	1.598	2	1.597	20
$\bar{2}62$	1.593						

* Cu/Ni radiation, diffractometer method, 0.5° min^{-1} in 2θ.
** Johan *et al.* (1974).
† Calculated from the single crystal data.

unknown Ag–Hg–As–S phase was usually observed.

Chemistry

Laffittite and synthetic laffittite were analyzed with an ARL-SEMQ electron microprobe using an operating voltage of 20 kV and a sample current of 0.15 μA. Wavelength scan of natural laffittite disclosed only Hg, Ag, As, and S in major amounts, and a minor amount of Sb. No other elements were present at levels detectable by microprobe analysis. Standards of marrite and livingstonite were used for quantitative analysis. The data were corrected using the MAGIC-4 computer program. The results are given in Table 2, together with the data given in the original description (Johan *et al.*, 1974).

Natural laffittite from the Getchell mine as well as synthetic laffittite have compositions practically identical with values reported by Johan *et al.* (1974). The only significant difference is the presence of antimony in appreciable amounts in our natural specimen. This fact may bear on the difference of the color between natural and synthetic crystals; the former are somewhat darker because of the presence of antimony impurity.

Laffittite is not readily soluble in HCl (1:1), HNO_3 (1:1) or NaOH (10%).

Crystal structure

Introduction

Laffittite, $AgHgAsS_3$, is classified among the sulfosalt minerals. Among the many known sulfo-

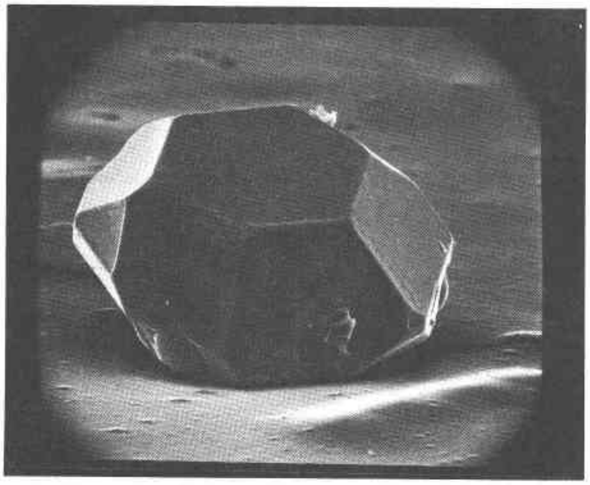

Fig. 2. Scanning electron micrograph of synthetic laffittite (80 × 60 × 30 μm).

salts, only a few are sulfosalts of mercury: for example livingstonite, $HgSb_4S_8$, christite, $TlHgAsS_3$ and vrbaite, $Hg_3Tl_4As_8Sb_2S_{20}$. A purpose of this study is to elucidate the crystal chemistry of this rare sulfosalt of mercury. Another interest is to clarify the structural relationship with marrite, $PbAgAsS_3$, with a chemical formula analogous to that of laffittite, $AgHgAsS_3$.

Experimental

A small single crystal with overall dimensions 90 × 50 × 70 μm was isolated from the Museum specimen (#134796). The shape of the crystal was irregular; however the extremely limited amount of material available precluded an attempt to grind a spherical specimen.

The unit cell parameters were refined by a least squares treatment of the setting angles of 15 reflections centered automatically on the Syntex $P2_1$ automatic diffractometer using monochromated Mo$K\alpha$ radiation ($\lambda = 0.70926$Å). Crystal data are as follows: $AgHgAsS_3$ FW = 479.56, space group Aa, $a = 7.732(3)$, $b = 11.285(7)$, $c = 6.643(4)$Å, $\beta = 115.16(3)°$, $Z = 4$, D(calc.) = 6.071 g/cm^3.

The intensities were measured on the Syntex $P2_1$ automatic diffractometer by the 2θ–θ method using Mo$K\alpha$ radiation ($\lambda = 0.70926$Å), graphite monochrometer, variable scan rate: slowest 2.02°/min., fastest 29.30°/min. and scan time/total background time ratio = 2. The intensities of three standard reflections were measured every 60 reflections. Although there was no large fluctuation of the intensities of standard reflections, the intensity data were corrected for fluctuations using the computer program DATCO5 (Stewart *et al.*, 1976). A total of 1509 reflections were observed, of which 937 reflections have a criteria $|F_o| \geq 3\ \sigma(|F_o|)$ and were used for subsequent crystal structure analysis. The intensities were corrected for Lorentz and polarization factors. An absorption correction was made in a late stage of structure determination.

Substructure relationship

The diffraction pattern of laffittite clearly indicated the presence of strong reflections when $l = 2p$, $k = 6q$ and $h = 2r$; $l = 2p + 1$, $k = 6q + 3$ and $h = 2r$, where p, q, and r are integers. These subcell reflections implied the presence of a face centered pseudo-cubic subcell with $a' = 5.394$, $b' = 5.394$, $c' = 6.102$Å, $\alpha' = 82.97$, $\beta' = 82.97$, and $\gamma' = 88.44°$. The transformation matrix from the true cell is given by:

$$a' = \tfrac{1}{2}a - \tfrac{1}{3}b,$$
$$b' = \tfrac{1}{2}a + \tfrac{1}{3}b,$$
$$c' = \tfrac{1}{2}a + c$$

Similar substructure relationships have been observed in structures of many sulfosalts such as marrite, $PbAgAsS_3$ (Wuensch and Nowacki, 1967), miargyrite, $AgSbS_2$ (Knowles, 1964) and smithite $AgAsS_2$ (Hellner and Burzlaff, 1964), where those structures are superstructures based upon the PbS (or rocksalt) structure type. Although the subcell of laffittite is significantly deformed compared with the true PbS structure (a = 5.96Å), the above observation implied that the structure of laffittite is closely related to the PbS structure type.

Structure determination and refinement

Normalized structure factors were calculated using NORMSF (Stewart *et al.*, 1972). Since the statistics of the E's did not indicate clearly the absence of a center of symmetry, the centrosymmetric space

Table 2. Electron microprobe chemical analyses of laffittite

	1	2	3	4
Ag	21.8	22.2	21.9	22.5
Hg	43.7	43.6	41.0	41.8
As	14.8	15.3	15.6	15.6
Sb	0.8	-	-	-
S	21.9	21.8	20.3	20.1
Total	103.0	102.9	98.8	100.0

1. Laffittite from Getchell mine.
2. Synthetic laffittite.
3. Laffittite from Jas Roux mine (Johan et al., 1974).
4. Theoretical $AgHgAsS_3$.

group *A*2/*a* was assumed for the structure analysis.

A three dimensional Patterson synthesis clearly indicated the cubic closest packing nature of the structure, *i.e.*, a PbS type structure. The space group *A*2/*a* with $Z = 4$ restricts the metal atoms to special positions, among which the "*e*" position of the Wyckoff notation was found to be suitable for metal atoms according to the Patterson maps. Thus metal atoms were considered to be located at (¼,*y*,0). The *y* coordinates of the metal atoms were obtained from the Harker section of the *a* glide plane. This revealed three most probable positions for the metal atoms. Because of the PbS-like nature of the structure, distribution of the three metal atoms among these three positions could not be determined from the Patterson maps.

A total of 6 models was considered to represent probable sets of the metal distributions. Determination of the correct configuration was achieved by systematic examination of all these possible sets. Several cycles of full-matrix least-square refinement (CRYLSQ, Stewart *et al.*, 1972) with the isotropic temperature factors were carried out using a limited number of reflections ($\sin\theta/\lambda < 0.7$, 609 reflections). The result indicated that one model seemed to be correct because it gave the lowest conventional *R* factor ($R = \Sigma||F_o| - |F_c||/\Sigma|F_o|$) of 0.25 and reasonable values of the temperature factors; the highest *R* factor was 0.32 among the 6 models. Fourier and difference syntheses were performed using this model to find the positions of the sulfur atoms. Although the Fourier maps showed several peaks which might correspond to the sulfur electron density, those positions were found to be unsatisfactory for the assumed space group *A*2/*a*, because their distribution did not support the presence of a 2-fold axis. This indicated that the structure was in fact acentric; hence the true space group has been taken to be *Aa*.

Introducing the new space group *Aa*, a systematic examination of the distribution of the metal atoms was again repeated by the full-matrix least-squares program. In this examination, the original 6 models were reconsidered for those metal positions had been located at four-fold sites in the former space group and the change of the space group from *A*2/*a* to *Aa* did not affect the multiplicity of the sites. The result showed that the first model was wrong, and a different model was chosen for its reasonable temperature factor and the lowest *R* factor of 0.20; the *R* factors of the other models varied from 0.22 to 0.27. Subsequent Fourier and difference syntheses gave several electron density peaks. Consideration of coordination environment around the metal atoms aided by bond distance calculation led to three appropriate positions for sulfur atoms. Three cycles of the full-matrix least-squares refinement of metal and sulfur coordinates with isotropic temperature factors reduced the *R* to 0.12. Two additional cycles of refinement with anisotropic temperature factors reduced *R* to 0.10.

The high absorption coefficient of laffittite ($\mu_{\mathrm{Mo}K\alpha} = 401.5\ \mathrm{cm}^{-1}$) necessitated an accurate correction for X-ray absorption; however, the correction was difficult because of the complex shape of the crystal. This was approximated by a collection of eight plane faces. The absorption correction program ABSORB (Stewart *et al.*, 1972) was applied: the number of sampling points was 1000; absorption correction factors A*: maximum 30.99 for (020), minimum 6.39 for ($\bar{1}$.18.4). Two further cycles of the full-matrix least-squares refinement with anisotropic temperature factors converged to $R = 0.072$. The absorption correction remarkably improved the agreement between F_o and F_c for the (0*k*0) reflections, but the correction is still only approximate because of the complex shape of the crystal.

All the scattering factors used in the structure factor calculation were taken from Cromer and Mann (1968), and anomalous dispersion from the

Table 3. Atomic parameters and thermal parameters with estimated standard deviations in parentheses

Atom	x	y	z	B*	U_{11}**	U_{22}	U_{33}	U_{12}	U_{13}	U_{23}
Ag	0.25	0.0221(4)	0	2.50(9)	291(22)	390(21)	326(23)	92(17)	152(21)	-47(18)
Hg	0.7891(6)	0.3166(2)	0.0249(9)	2.09(3)	303(8)	280(8)	292(8)	-46(11)	165(7)	52(10)
As	0.2874(11)	0.3523(3)	0.0195(12)	1.11(6)	137(14)	175(16)	162(17)	-45(25)	79(13)	-139(21)
S(1)	0.4214(15)	0.0089(9)	0.4318(18)	1.19(14)	197(37)	168(40)	171(36)	6(32)	128(32)	0(31)
S(2)	0.9828(15)	0.2841(9)	0.4697(18)	1.15(14)	178(37)	185(40)	116(33)	-11(32)	73(30)	-1(31)
S(3)	0.4369(16)	0.3722(10)	0.3947(18)	1.28(15)	214(43)	235(44)	109(35)	-30(35)	93(34)	24(32)

* Isotropic temperature factors are from the last cycle of refinement before changing to anisotropic temperature factors.

** Form of the anisotropic temperature factor: $\exp[(-2\P^2)(10^{-4})(U_{11}h^2a^{*2} + \cdots\cdots + 2U_{23}klb^*c^*\cos\alpha^*)]$.

Table 5. Interatomic distances (Å) and bond angles (°) with estimated standard deviations in parentheses

Distances (A)					
Ag - S(3)	2.510(13)	Hg - S(1)	2.417(13)	As - S(1)	2.247(14)
- S(3')	2.516(12)	- S(2)	2.509(12)	- S(3)	2.269(13)
- S(1)	2.602(11)	- S(2')	2.710(12)	- S(2)	2.277(14)
- S(2)	2.894(12)	- S(3)	2.727(13)	- S(1')	3.066(14)
- S(2')	3.342(12)	- S(1')	3.418(12)	- S(2')	3.488(12)
- S(1')	3.560(10)	- S(3')	3.955(11)	- S(3')	3.541(13)

Angles (°)					
S(3) - Ag - S(3')	147.3(3)	S(1) - Hg - S(2)	143.8(4)	S(1) - As - S(3)	97.5(5)
S(3) - Ag - S(1)	100.7(3)	S(1) - Hg - S(2')	107.0(3)	S(1) - As - S(2)	95.0(6)
S(3) - Ag - S(2)	92.4(4)	S(1) - Hg - S(3)	106.0(5)	S(1) - As - S(1')	92.2(4)
S(3) - Ag - S(2')	81.7(4)	S(1) - Hg - S(1')	81.2(3)	S(1) - As - S(2')	94.7(4)
S(3) - Ag - S(1')	82.8(3)	S(1) - Hg - S(3')	77.0(3)	S(1) - As - S(3')	153.3(4)
S(3') - Ag - S(1)	108.2(4)	S(2) - Hg - S(2')	98.5(4)	S(3) - As - S(2)	99.6(5)
S(3') - Ag - S(2)	100.1(4)	S(2) - Hg - S(3)	95.5(4)	S(3) - As - S(1')	99.0(5)
S(3') - Ag - S(2')	82.4(3)	S(2) - Hg - S(1')	66.4(3)	S(3) - As - S(2')	166.9(6)
S(3') - Ag - S(1')	65.4(3)	S(2) - Hg - S(3')	74.6(3)	S(3) - As - S(3')	108.1(5)
S(1) - Ag - S(2)	94.6(3)	S(2') - Hg - S(3)	97.4(3)	S(2) - As - S(1')	159.0(4)
S(1) - Ag - S(2')	91.9(3)	S(2') - Hg - S(1')	108.4(4)	S(2) - As - S(2')	83.9(4)
S(1) - Ag - S(1')	164.3(4)	S(2') - Hg - S(3')	171.2(4)	S(2) - As - S(3')	88.4(4)
S(2) - Ag - S(2')	172.0(3)	S(3) - Hg - S(1')	150.2(3)	S(1') - As - S(2')	75.9(3)
S(2) - Ag - S(1')	100.7(3)	S(3) - Hg - S(3')	88.9(3)	S(1') - As - S(3')	76.6(3)
S(2') - Ag - S(1')	73.3(3)	S(1') - Hg - S(3')	64.0(3)	S(2') - As - S(3')	59.2(3)

International Tables for X-ray Crystallography (1974). Computer programs of the X-RAY SYSTEM were used throughout the calculations (Stewart *et al.*, 1972 and 1976). Final atomic parameters are given in Table 3. The observed and calculated structure factors are deposited as Table 4.[2]

Description of the structure

A projection of the structure down the a^* axis is presented in Figure 3. Metal and sulfur atoms form a puckered hexagonal ring of $AgHgAsS_3$. The hexagonal rings link to each other by sharing all edges, forming a sheet parallel to (100). Those sheets link up and down by Hg–S and Ag–S bonds. The distribution of metal and sulfur atoms is closely related to the PbS structure. Although the distortion from the true PbS structure is large, the metal atoms are basically located in octahedral sites formed by cubic close-packing-like arrangement of the sulfur atoms (Table 5). The (200) plane corresponds to the (111) plane of the PbS structure.

Figure 4 is a projection of the structure viewed along the c^* axis. The laffittite structure can now be described in another way. The figure shows two kinds of rings: one is a six membered ring of Ag_2HgS_3 and the other is a zig-zag ten membered ring of $AgHg_2As_2S_5$. A combination of the two rings composes a sheet parallel to (001). The sheets link to each other by the metal sulfur bonds in the [001] direction. The figure also indicates the stacking manner of the hexagonal $AgHgAsS_3$ rings.

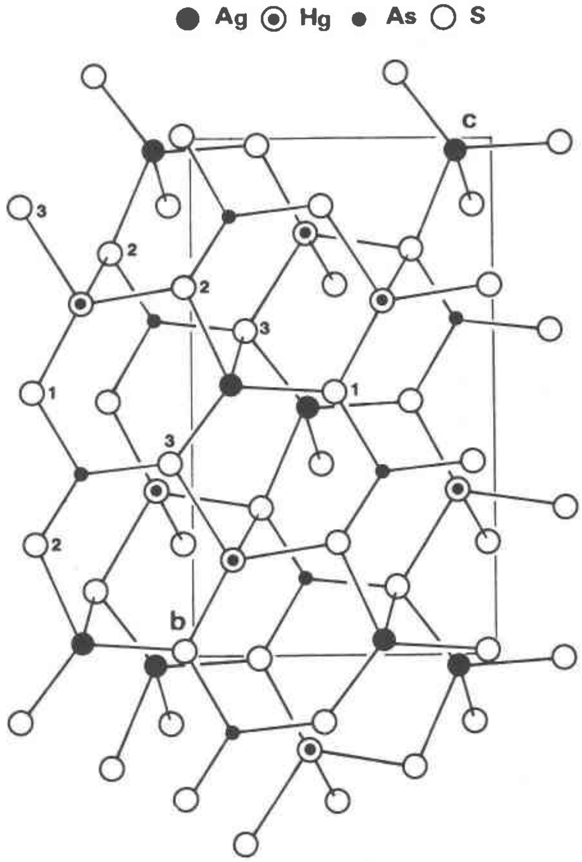

Fig. 3. A view of the laffittite structure projected along the a^* axis.

---

[2] Table 4 may be obtained by ordering Document AM-82-210 from the Business Office, Mineralogical Society of America, 2000 Florida Ave., N.W., Washington, D. C. 20009. Please remit $1.00 in advance for the microfiche.

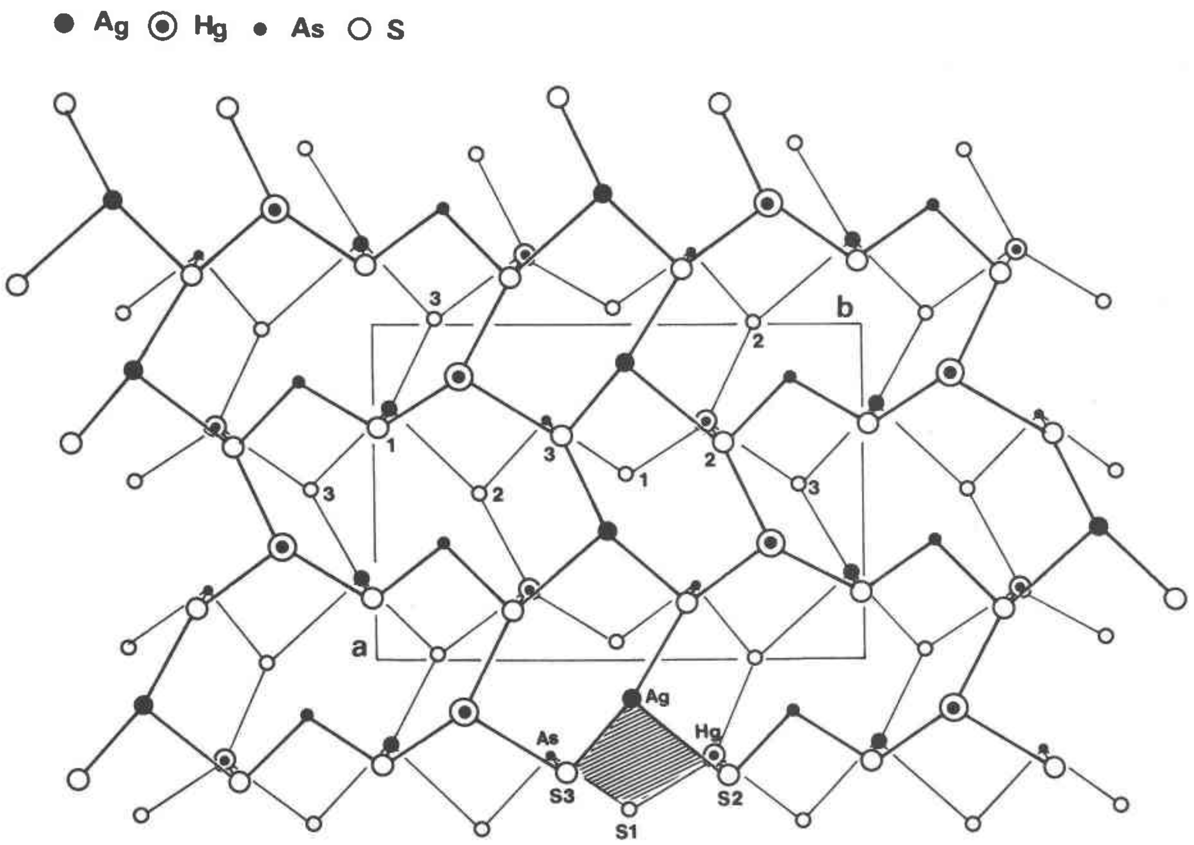

Fig. 4. Projection of the laffittite structure viewed along the c^* axis. Atoms near $z = 1/2$ are drawn by larger symbols than those near $z = 0$. The hexagonal ring of $AgHgAsS_3$ observed in Fig. 1 is marked by the shaded lines for comparison.

As we observe here, the structure of laffittite is in fact a three dimensional network. The AsS_3 pyramids are isolated from each other in the structure; hence the structure is classified into the category IIa_1 of the sulfosalt classification suggested by Nowacki (1969, 1970).

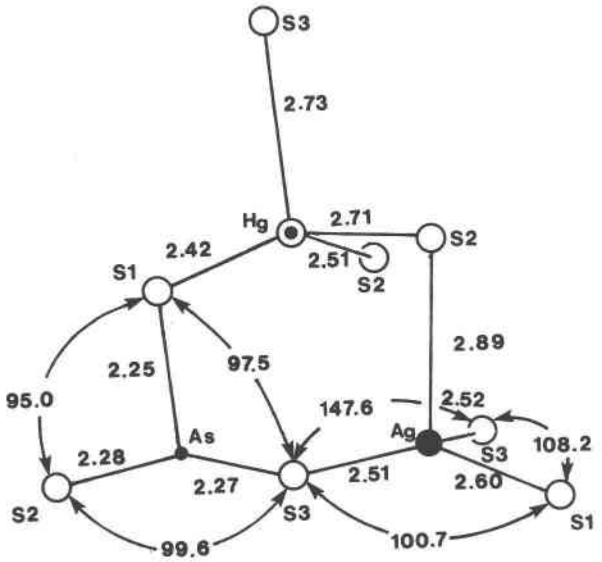

Fig. 5. Coordination about the metal atoms with selected bond lengths and angles (bond angles are marked by arrows).

Bond distances and angles

Interatomic distances and bond angles are given in Table 5. Selected bond lengths and angles are illustrated in Figure 5. Coordination around the metal atoms is typical for sulfosalt structures. The As atom exhibits the usual three-fold coordination by S, with As situated at one vertex of a trigonal pyramid. As–S bond distances range from 2.247 to 2.277Å with an average of 2.26Å. These values are comparable with those of marrite, $PbAgAsS_3$: 2.259–2.279Å (Wuensch and Nowacki, 1967); christite, $HgTlAsS_3$: 2.232–2.258Å (Brown and Dickson, 1976); and trechmannite, $AgAsS_2$: 2.218–2.308Å (Matsumoto and Nowacki, 1969). The average As–S bond distance of 2.26Å agrees very well with the non-bridging bond distance of 2.26Å for the AsS_3 pyramid given by Takeuchi and Sadanaga (1969). The three As–S bonds are nearly orthogonal and range from 95.0 to 99.6° indicating the p-orbital

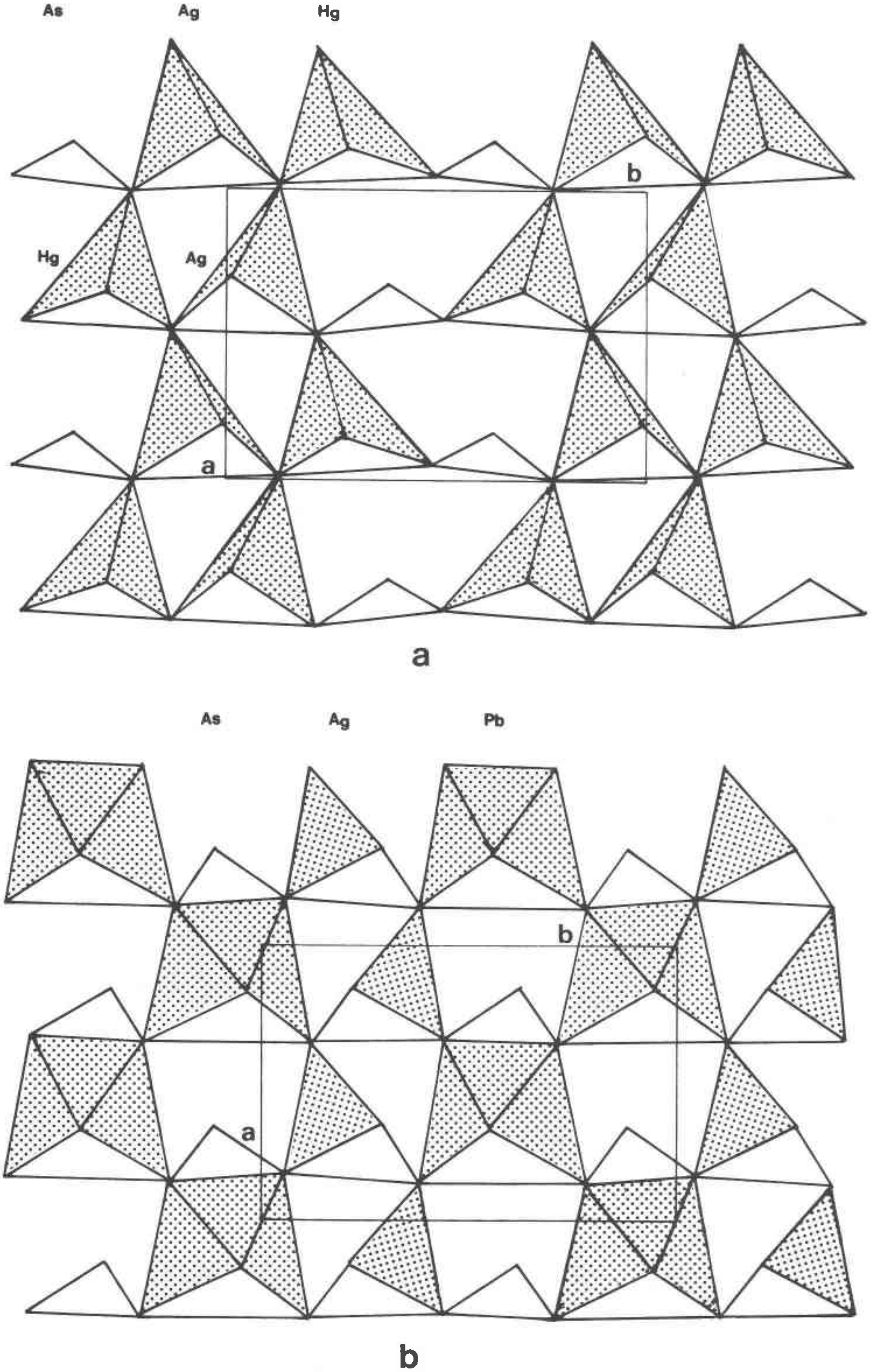

Fig. 6. Linkage in (001) of the coordination polyhedra formed by the arrangement of sulfur atoms about metal atoms: (a) laffittite, (b) marrite.

nature of the bonds. The additional neighbors of the As atom are three S atoms at significantly larger distance from 3.066 to 3.541Å. As a result, the S atoms exhibit a distorted octahedral coordination about the As atoms. This configuration leaves a cavity for the unshared electron pair of arsenic.

The Ag atom has three nearest S neighbors at distances 2.510, 2.516, and 2.602Å, and one farther at 2.894Å. The three nearest S atoms form a nearly planar trigonal coordination; the sum of the three angles is 356.5°. This (3 + 1)S coordination of Ag is widely observed in other sulfosalts of silver such as smithite, $AgAsS_2$ (Ag–S = 2.51, 2.56, 2.68, 2.84; 2.52, 2.55, 2.65, 2.90Å; Hellner and Burzlaff, 1964), miargyrite, $AgSbS_2$ (Ag–S = 2.44, 2.50, 2.58, 2.72Å; Knowles, 1964), hatchite, $PbTlAgAs_2S_5$ (Ag–S = 2.48, 2.52, 2.54, 2.93Å; Marumo and Nowacki, 1969) and freieslebenite, $PbAgSbS_3$ (Ag–S = 2.522, 2.575, 2.687, 2.928Å; Ito and Nowacki, 1974).

The Hg atom exhibits a distorted tetrahedral coordination by S, with two S atoms at 2.417 and 2.509Å, and two farther at 2.710 and 2.727Å. The most common coordination of Hg atoms by S atoms is an approximately linear linkage of closest neighbors. This kind of configuration is observed in cinnabar, HgS (Hg–S = 2.36Å, S–Hg–S = 172°, Aurivillius, 1950), in livingstonite, $HgSb_4S_8$ (Hg–S = 1.90Å, S–Hg–S = 179.1°; Hg′–S = 2.52Å, S–Hg′–S = 180.0°; Srikrishnan and Nowacki, 1975), in vrbaite $Hg_3Tl_4As_8Sb_2S_{20}$ (Hg–S = 2.38Å, S–Hg–S = 166.0°; Ohmasa and Nowacki, 1971) and many other mercury compounds. Some mercury compounds are known to have tetrahedral coordination of Hg by S, in which there are two kinds of configurations: one is Hg surrounded by 4S at about equal distances, while the other is Hg surrounded by 2S at short distances and 2S at long distances, *i.e.* (2+2)S coordination. The former examples include metacinnabarite, HgS (Hg–S = 2.55Å; Buckley and Vernon, 1925), vrbaite (Hg–S = 2.570 and 2.581Å; Ohmasa and Nowacki, 1971) and galkhaite, $Hg_{12}Tl(AsS_3)_8$ (Hg–S = 2.503Å; Divjaković and Nowacki, 1975), while the latter is seen in the structure of christite $HgTlAsS_3$ (Hg–S = 2.460, 2.471, 2.646, and 2.661Å; Brown and Dickson, 1976). Laffittite belongs to the latter group. The average tetrahedral Hg–S bond distances in both groups are about equal: metacinnabarite 2.55, vrbaite 2.58, galkhaite 2.50, christite 2.56, and laffittite 2.59Å. The observed (2 + 2)S coordination may be explained as a result of distortion from the ideal tetrahedral coordination of sp^3 type due to stereochemical effects of neighboring atoms.

Structural relationship with marrite, $PbAgAsS_3$

Laffittite is compositionally related to marrite; the Pb atom can be tentatively considered to be substituted by the Hg atom in laffittite. The crystal structure of marrite is also a superstructure based upon the PbS structure type (Wuensch and Nowacki, 1967). Therefore it is interesting to look for a structural relationship between the two minerals.

Figure 6 shows the linkage in (001) of the coordination polyhedra formed by the arrangement of S atoms about (a) metal atoms near $z = 0$ in laffittite and (b) metal atoms near $z = 3/4$ in marrite. The linkage of polyhedra appears to be topologically different because of the difference of coordination around Hg and Pb atoms; *i.e.*, Hg forms a tetrahedral coordination polyhedron, while Pb forms an octahedral one. However, the distribution of metal atoms is found to be similar between the two structures if we consider the Hg atom to be equivalent to the Pb atom. Laffittite belongs to space group *Aa*, marrite to $P2_1/a$. Both structures have the same *a* glide plane, and the translation by the *A*-centered cell in laffittite is substituted by the two-fold screw axis in marrite. Thus we see the structure of laffittite is closely related to that of marrite.

Acknowledgments

Intensity data for the crystal structure analysis were collected at the National Bureau of Standards by courtesy of Dr. Judith Stalik. Her kind help in data collection is greatly appreciated. The authors are grateful to Dr. Masaaki Shimizu for his advice in optical measurements, Mr. Timothy O'Hearn for his translation of the French literature, and Mr. Richard Johnson for preparation of microprobe specimens. The senior author is indebted to the Smithsonian Institution for a grant of a Predoctoral Fellowship. He is grateful to Prof. Kozo Nagashima and Dr. Akira Kato for their kind encouragement.

References

Aurivillius, K. L. (1950) On the crystal structure of cinnabar. Acta Chemica Scandinavica, 4, 1413–1436.

Brown, K. L. and Dickson, F. W. (1976) The crystal structure of synthetic christite $HgTlAsS_3$. Zeitschrift für Kristallographie, 144, 367–376.

Buckley, H. E. and Vernon, W. S. (1925) The crystal structures of the sulphides of mercury. Mineralogical Magazine, 20, 382–392.

Cromer, D. T. and Mann, J. B. (1968) X-ray scattering factors computed from numerical Hartree Fock functions. Acta Crystallographica, 25, 321–323.

Divjaković, V. and Nowacki, W. (1975) Die Kristallstruktur von

Galchait $[Hg_{0.76}(Cu,Zn)_{0.24}]_{12}Tl_{0.96}(AsS_3)_8$. Zeitschrift für Kristallographie, 142, 262–270.

Hellner, E. and Burzlaff, H. (1964) Die Struktur des Smithits $AgAsS_2$. Naturwissenschaften, 51, 35–36.

International Tables for X-ray Crystallography, Vol. IV (1974) Kynoch Press, Birmingham, England.

Ito, T. and Nowacki, W. (1974) The crystal structure of freieslebenite, $PbAgSbS_3$. Zeitschrift für Kristallographie, 139, 85–102.

Johan, Z., Mantienne, J. and Picot, P. (1974). La routhiérite, $TlHgAsS_3$ et la laffittite, $AgHgAsS_3$, deux nouvelles espèces minérales. Bulletin de la Société française de Minéralogie et de Cristallographie, 97, 48–53.

Knowles, Ch. R. (1964) A redetermination of the structure of miargyrite, $AgSbS_2$. Acta Crystallographica, 17, 847–851.

Marumo, F. and Nowacki, W. (1967) The crystal structure of hatchite $PbTlAgAs_2S_5$. Zeitschrift für Kristallographie, 125, 249–265.

Matsumoto, T. and Nowacki, W. (1969) The crystal structure of trechmannite, $AgAsS_2$. Zeitschrift für Kristallographie, 129, 163–177.

Nowacki, W. (1969) Zur Klassifikation und Kristallchemie der Sulfosalze. Schweizerische Mineralogische und Petrographische Mitteilungen, 49, 109–156.

Nowacki, W. (1970) Zur Klassifikation der Sulfosalze. Acta Crystallographica, B26, 286–289.

Ohmasa, M. and Nowacki, W. (1971) The crystal structure of vrbaite $Hg_3Tl_4As_8Sb_2S_{20}$. Zeitschrift für Kristallographie, 134, 360–380.

Stewart, J. M., Kruger, G. J., Ammon, H. L., Dickinson, C. W., and Hall, S. R. (1972) The X-RAY SYSTEM, Version of 1972. Technical Report TR-192. Computer Science Center. University of Maryland, College Park, Md.

Stewart, J. M., Machin, P. A., Dickinson, C. W., Ammon, H. L., Heck, H., and Flack, H. (1976) The X-RAY SYSTEM, Version of 1976. Technical Report TR-446. Computer Science Center. University of Maryland, College Park, Md.

Srikrishnan, T. and Nowacki, W. (1975) A redetermination of the crystal structure of livingstonite $HgSb_4S_8$. Zeitschrift für Kristallographie, 141, 174–192.

Takeuchi, Y. and Sadanaga, R. (1969) Structural principles and classification of sulfosalts. Zeitschrift für Kristallographie, 130, 346–368.

Wuensch, B. J. and Nowacki, W. (1967) The crystal structure of marrite, $PbAgAsS_3$. Zeitschrift für Kristallographie, 125, 459–488.

Manuscript received, January 26, 1982;
accepted for publication, June 21, 1982.